ELSEVIER

PII: S0032-3861(97)10138-0

Polymer Vol. 39 No. 19, pp. 4599–4608, 1998
© 1998 Elsevier Science Ltd
Printed in Great Britain. All rights reserved
0032-3861/98/$19.00+0.00

Phase transitions, structure evolution, and mechanical properties of blends of two crystalline polymers: poly(vinylidene fluoride) and poly(butylene adipate)

Irada Isayeva[a], Thein Kyu[a,*] and R. St. John Manley[b]
[a]*Institute of Polymer Engineering, The University of Akron, Akron, OH 44325, USA*
[b]*Department of Chemistry, McGill University, Montreal, Quebec, Canada H3A 2A7*
(Received 24 June 1997; revised 11 August 1997; accepted 12 August 1997)

The emergence of crystalline structures during phase transitions, involving crystallization and phase separation in blends of poly(vinylidene fluoride) (PVF_2) and poly(butylene adipate) (PBA) has been examined by means of time-resolved depolarized light scattering, polarizing optical microscopy, and differential scanning calorimetry. These PVF_2/PBA blends are known to exhibit various phase transitions including liquid–liquid phase separation, melting of the PVF_2, melting of the PBA, and a single glass transition, in the order of descending temperature. Several thermal quench experiments were undertaken, from the isotropic melt (200°C) to various crystallization temperatures at several blend compositions, to elucidate the emerging morphology and the crystallization kinetics in competition with phase separation. The development of the crystalline morphology is shown to be strongly dependent on the blend composition and crystallization temperature. Of particular interest is the observation that at PBA-rich compositions, nematic mesophase structures are formed even though the constituents do not contain mesogenic groups. Samples quenched from the isotropic melt (200°C) to low temperatures (e.g., 25°C) develop interconnected spinodal decomposition textures, and this observation is discussed in relation to the possible existence of an upper critical solution temperature (UCST). Tensile properties of high temperature crystallized blends with a spherulitic morphology have been compared with those of the thermal quenched blends having a periodic modulated crystalline structure. It is concluded that the mechanical properties are strongly dependent on the complex interplay of crystalline structure and phase-separated blend morphology. © 1998 Elsevier Science Ltd. All rights reserved.

(Keywords: crystalline polymer blends; phase transitions; structure evolution)

INTRODUCTION

Blends of two semicrystalline polymers are complex systems that offer interesting possibilities for studying the relation between phase behaviour and structure development in polymeric mixtures. In a recent series of papers[1,2], we have described the miscibility phase behaviour and crystallization in mixtures of poly(vinylidene fluoride) (PVF_2) and poly(1,4 butylene adipate) (PBA). Several phase transitions were observed in this blend system: a glass transition, melting of the PBA, melting of the PVF_2, and a lower critical solution temperature (LCST) type coexistence curve, in ascending order of temperature. Both blend components are semicrystalline at room temperature over the whole composition range. The observation of two melting transitions corresponding to those of the constituents, and the observed dual peaks (i.e., two distinct long periods) in the small-angle X-ray scattering experiment suggest that crystallization takes places separately in the blends at the length scale of crystalline lamellae[3], but the two crystalline phases co-exist within the same spherulites. The observations of a single glass transition in all blends, as well as the fact that the equilibrium melting point of the higher melting component (PVF_2) is lowered upon mixing with PBA, have been interpreted as suggestive of the miscible character of these blends in the amorphous phase.

Addition of PBA depresses the spherulitic growth and the overall crystallization rate of PVF_2. During the crystallization of PBA, the presence of the spherulitic microstructure of PVF_2 strongly influences the crystallization behaviour and morphology of PBA. In contrast to the bulk crystallization behaviour of the neat PBA, the development of spherulitic morphology is not observed in the high PBA blends. Crystallization of PBA in the blends initially takes place at the boundaries of the PVF_2, but at longer crystallization times, the crystal growth front of the PBA propagates toward the centre of the PVF_2 spherulites.

It is of interest to supplement the work described above with real time light scattering measurements so as to obtain information regarding the dynamics of structure formation. This study may be accomplished by transferring the system from one point of the phase diagram to another, e.g., quenching from the unstable region within the spinodal envelope (above the LCST) to a temperature below crystallization temperatures. Alternatively, T quench may be undertaken from a single isotropic melt state (below the LCST) to a temperature below the melting curve of PVF_2, but above that of the PBA, or by quenching directly below the crystallization temperatures of PBA. In those cases, the coupling of demixing and crystallization can occur and the competition between these two non-equilibrium phenomena may produce important new structures beyond those reported by Tanaka and Nishi[4,5]. For such experiments, a

* To whom correspondence should be addressed

detailed understanding of the liquid–liquid phase separation behaviour of the system is desirable. Accordingly, we have investigated the dynamics of liquid–liquid phase separation following a temperature jump from the isotropic melt to various temperatures above the LCST[6]. The results of the time evolution of structure factors were analysed in the context of non-linear and dynamical scaling theories of spinodal decomposition.

In this paper, we focus on the time-resolved light scattering study on structure evolution and crystallization behaviour in relation to mechanical properties of the PVF_2/PBA blends prepared by slow cooling, as well as by thermal quenching from the isotropic melt (200°C) to various temperatures below the crystallization temperatures of the constituents. At the middle and high PVF_2-rich compositions, the crystallization of PVF_2 spherulites is dominant. In high PBA-rich compositions, nematic line disclinations emerge although the PVF_2/PBA blends themselves contain no identifiable mesogenic groups. This nematic mesophase structure has been attributed to a consequence of specific interaction between the C-F groups of PVF_2 and carbonyl functionality of PBA[2]. The possible existence of an upper crystal solution temperature (UCST) below the crystallization temperatures of the blends has been postulated. The relationship between the emerging crystalline blend morphology and tensile properties of these blends has been presented.

EXPERIMENTAL SECTION

Poly(vinylidene fluoride) (PVF_2) was purchased from Polysciences Inc. (Warrington, PA), having a weight average molecular weight (M_w) of 140 000 and poly(butylene adipate) (PBA) ($M_w = 14\,000$), was obtained from Scientific Polymer Products Inc. (Ontario, NY). The as-received PBA and PVF_2 were dissolved in dimethyl formamide (DMF) in various proportions at a polymer concentration of 5 wt%. For differential scanning calorimetry (DSC) studies, the blends were precipitated in a non-solvent such as methanol and washed several times. The precipitates were dried in a vacuum oven for 4 days at ambient temperature. For optical and light scattering studies, blend specimens were solution cast via evaporation and dried under vacuum for 3 days. All specimens were preheated to 200°C for 30 min and quenched to room temperature prior to experiments.

DSC scans were undertaken on a Perkin-Elmer (DSC 7) from 200°C to room temperature under nitrogen circulation. The cooling rate was 1°C/min. An indium standard was used for temperature calibration. Using a one-dimensional silicon diode array (1024 pixels) Reticon camera interlinked with an Optical Multichannel Analyser (OMA III), time-resolved light scattering was carried out. A polarizing light microscope (Nikon Optiphot 2-pol) equipped with a Nikon camera (FX-35DX) was used for identifying temporal evolution of the phase-separated crystalline morphology. A temperature controller (Central Processor, FP 90, Mettler Co.) was used along with a sample hot stage (FP 82 HT, Mettler Co.) for heating specimens in the optical microscopic investigations.

Cylindrical dumbbell shape blend specimens were prepared by melt-mixing the constituents at 210°C for 3–5 min in a mini-Max mixer/moulder depending on composition and subsequently injection-moulded into a hot cylindrical mould controlled at various temperatures (about 200°C). Two types of blend samples were prepared: the first type was quenched from 200°C to room temperature to produce a bicontinuous spinodal structure. The second type was prepared by cooling the mould to 150°C and annealing at that temperature for 1 h to generate the spherulitic morphology. To investigate the effect of crystallization temperature, annealing was also performed at 130 and 110°C. A typical dumbbell shape specimen has a dimension of about 1.6 mm in diameter and 6–7 mm in gauge length. Tensile properties of the blends were measured by using a Monsanto tensile tester (Model T 10) at a cross-speed of 1 mm/min. All tensile measurements were performed at ambient temperature and the data were the average of at least five runs.

RESULTS AND DISCUSSION

Crystallization and structure formation

To better understand the emergence of the complex crystalline morphology in the PVF_2/PBA blends, several experiments were conducted from a single miscible state to the segregated crystalline states at a predetermined cooling rate (i.e., 1°C/min). *Figure 1* shows that the development of crystalline textures in the blends is strongly composition dependent. In a PVF_2-rich blend such as the 90/10 composition, tiny typical-type PVF_2 spherulites develop and grow rapidly until they impinge into each other. In the 50/50 blend, the spherulites of PVF_2 are significantly larger since fewer nuclei are formed at elevated crystallization temperatures, thereby permitting PVF_2 crystals to grow in the continuum of PBA melt. During crystallization, PVF_2 spherulites reject PBA molecules to the spherulitic boundaries, exhibiting an irregular texture at the interstitial region of the spherulites. With continued cooling below the crystallization temperature of PBA, crystallization of the PBA phase takes place from the periphery toward the centre of the PVF_2 spherulites. In the blends rich in PBA such as the 20/80 PVF_2/PBA, the spherulitic texture is highly disordered resembling a sheaf-like texture. In the 10/90 PVF_2/PBA blend, the structure is reminiscent of a nematic

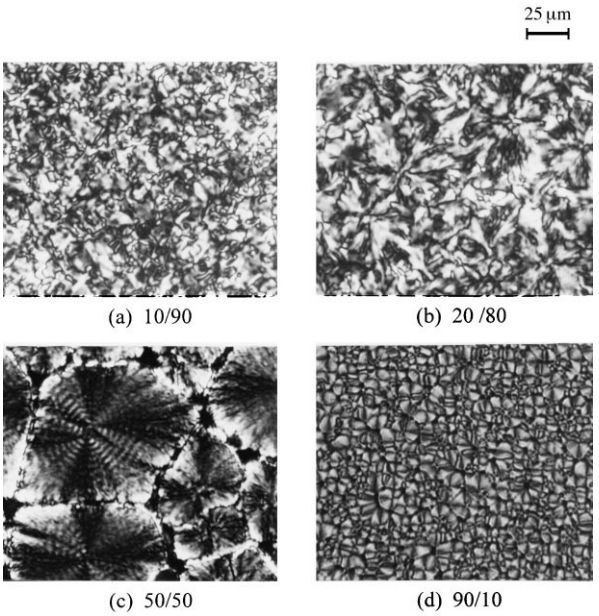

Figure 1 Polarized optical micrographs (under crossed Nicols) displaying various crystalline textures in PVF_2/PBA blends of various compositions after cooling from 200°C to room temperature, exhibiting (a) Schlieren texture in the 10/90 PVF_2/PBA blend; (b) sheaf-like incomplete spherulites in the 20/80 blend; (c) large spherulites with concentric rings in the 50/50 blend; and (d) α type spherulites in the 90/10 blend

mesophase structure with a multitude of line disclinations, although the constituents contain no mesogenic groups. The observed mesophase structure in a non-mesogenic mixture appears unique, but it bears a striking resemblance to the mesophase structure observed in a non-mesogenic polymer blend, where strong hydrogen bonding can occur[7,8]. According to Talroze *et al.*[8] the strong hydrogen bonding can be used as a means of generating a LC mesophase phase in polyacrylic acid/amine chloride complexes. The present PVF_2/PBA blend has been shown to have some specific interaction between the C-F group of PVF_2 and the carbonyl group of PBA[2]. Hence, the observed mesogenic texture in this PVF_2/PBA mixture perhaps points to the same phenomenon of nematic-like ordering in the non-mesogenic blends. (Note that liquid crystals having orientational ordering without positional ordering are called nematics.)

The progression of structure development from rod-like fibrils to a sheaf-like texture and eventually to a spherulitic LC texture with multiple line disclinations can be discerned in the 10/90 PVF_2/PBA during the course of cooling (*Figure 2a*). The sheaf and spherulitic structures in the 20/80 composition (*Figure 2b*) appear more regular relative to those of the 10/90 PVF_2/PBA blend. In the case of 50/50 composition, large spherulitic structures develop and grow with time until these spherulites impinge on each other (*Figure 2c*). When the temperature is lowered below the crystallization temperature of PBA (e.g. 42°C), the rejected PBA chains crystallize at the periphery of the spherulites. As shown in *Figure 2d*, multiple tiny spherulites develop in

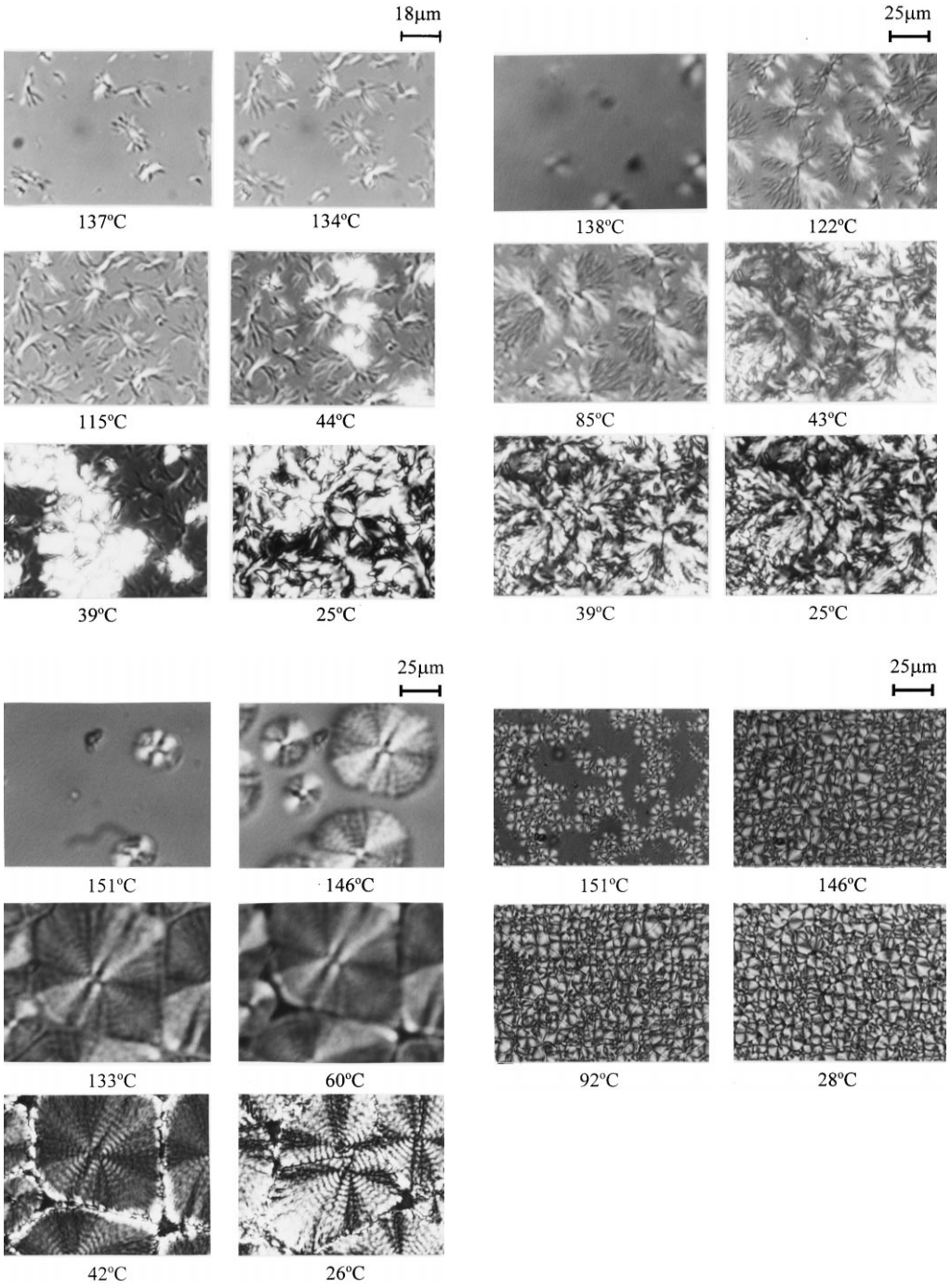

Figure 2 Optical micrographs (under crossed polars) showing the emergence of crystalline texture as a function of temperature during the course of cooling from 200°C to ambient temperature: (a) 10/90; (b) 20/80; (c) 50/50; and (d) 90/10 PVF_2/PBA. The cooling rate was 1°C/min

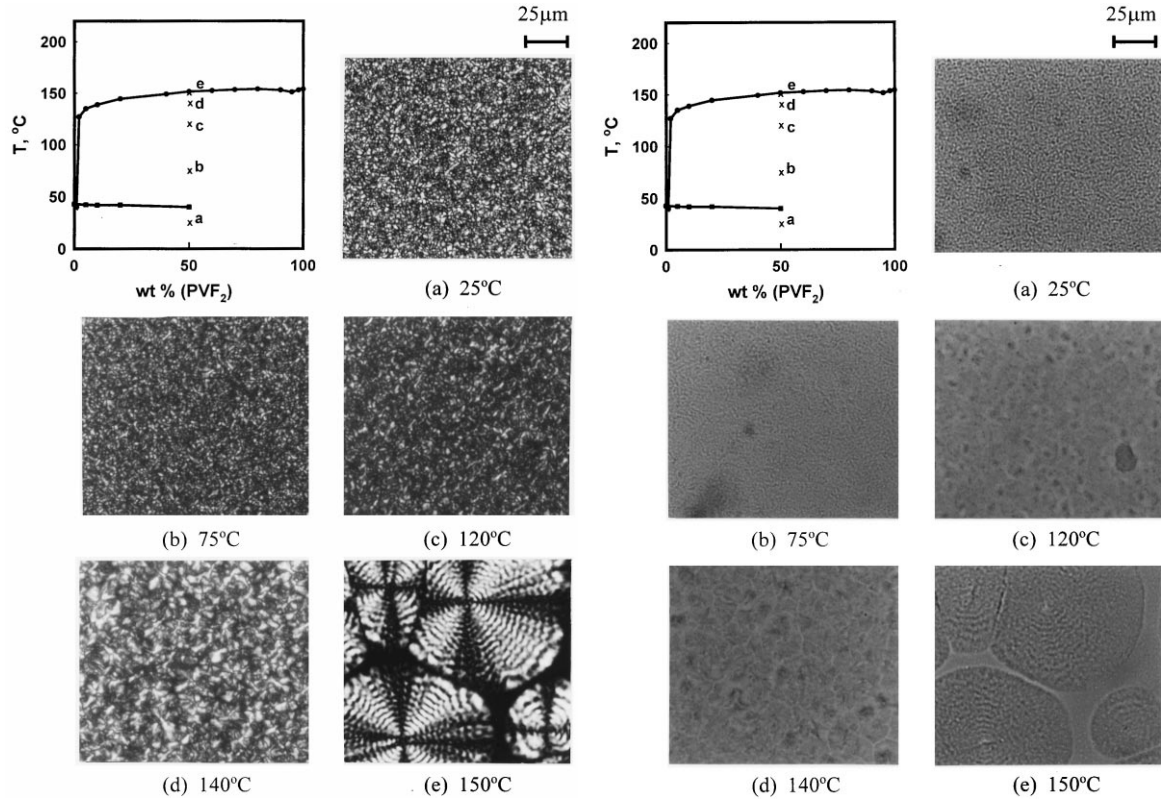

Figure 3 Optical micrographs obtained at the 50/50 PVF_2/PBA blend after quenching from 200°C to several temperatures: (a) under crossed polars displaying the crystalline morphologies; and (b) unpolarized condition exhibiting phase-separated domains. The small figure in the upper-left corner is to indicate the positions of temperatures to which the samples were quenched from the isotropic melt of 200°C with reference to the phase diagram. The crystallization curves were obtained at 1°C/min

the case of PVF_2-rich 90/10 composition, and rapidly fill the whole sample space, which is often called 'volume filling' until these spherulites impinge into each other[9]. From the foregoing it is evident that the crystalline morphologies of these PVF_2/PBA blends display not only composition dependence, but also strong temperature dependence.

Figure 3a and *b* show the evolution of spherulitic texture in the 50/50 blend following a temperature quench from isotropic melt (200°C) to various crystallization temperatures under (a) polarized under crossed polarizers; and (b) unpolarized conditions. Tiny multiple spherulites appear at low temperature quenches to 25 and 75°C, whereas large spherulites can be discerned at a high temperature of 150°C. The general trend is that the larger the T quench (supercooling), the smaller the length scale or the average spherulitic size[10]. In the unpolarized configuration, the T quenches to low temperatures such as 25 and 75°C manifest interconnected structures suggestive of spinodal decomposition (SD). At intermediate temperatures of 120 and 140°C, the structure is coarser. The observed SD structure is a signature of liquid–liquid phase separation[11]. At 150°C, spherulites with a concentric ring pattern are clearly discernible. Moreover, the modulated SD structure is identifiable in the matrix as well as within these spherulites. It appears that liquid–liquid equilibrium probably exists below the crystallization temperatures of the PVF_2/PBA blends. A similar interconnected structure can be discerned in other compositions such as 90/10 (*Figure 4*) and 20/80 (*Figure 5*) under the unpolarized condition during thermal quenching from the isotropic melt of 200°C to room temperature. The modulated structures are birefringent, suggesting that crystallization occurs within these phase-separated structures. As shown in *Figure 4a*, the multiple

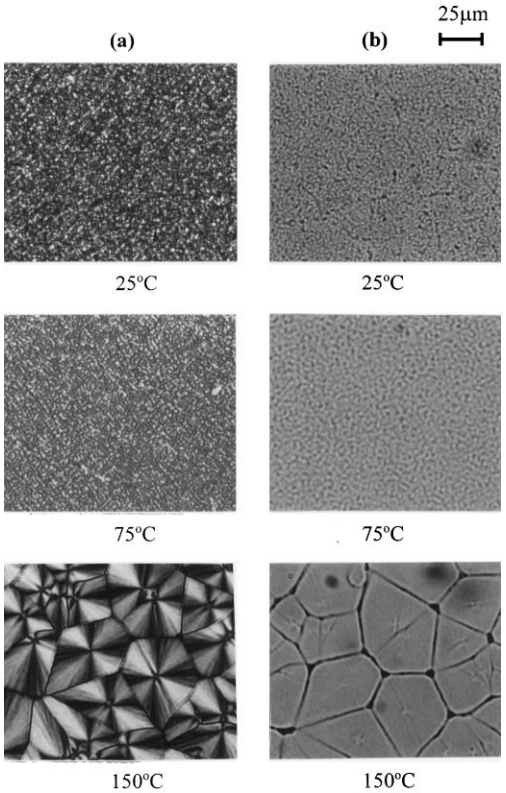

Figure 4 Optical micrographs obtained for the 90/10 PVF_2/PBA composition after quenching from 200°C to the indicated temperatures under: (a) cross-polarized condition showing crystalline textures; and (b) unpolarized condition showing phase-separated domain structure. Notice that there is no phase separation at 150°C

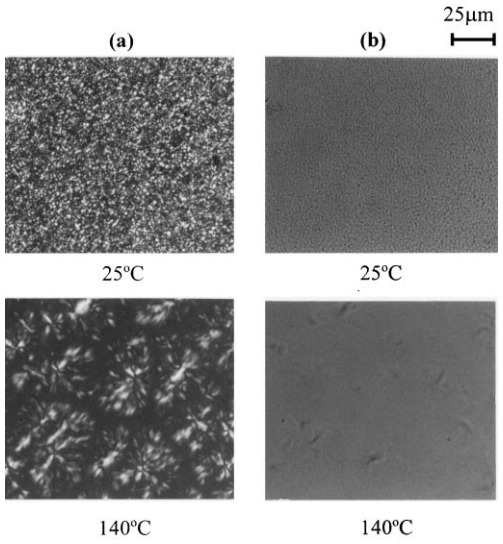

Figure 5 Optical micrographs obtained for the 20/80 PVF_2/PBA composition after quenching from 200°C to the indicated temperatures: (a) cross-polarized condition showing crystalline textures; and (b) unpolarized condition showing phase-separated domain structure. Notice that there is no phase separation at 140°C

tiny spherulitic morphology of the 90/10 PVF_2/PBA blend at 150°C is an α type crystal form of PVF_2 without any indication of the phase-separated structure, whereas at 75°C the modulated two-phase structure can be discerned (*Figure 4b*). In the case of 150°C, large spherulitic structures can be seen, but there is no discernible modulated structure. However, such a modulated structure is clearly identifiable in the 75°C case. Hence, the coexistence point for the 90/10 PVF_2/PBA would, if it exists, be located in between 150 and 75°C. In the case of the blends with 20% or lower PVF_2 content, crystallization of the PVF_2 phase occurs around 120–140°C without involvement of liquid–liquid phase separation. The two-phase structure is seen only when the temperature is lowered below the crystallization temperature of PBA, which is about 42°C (*Figure 6*). However, in the 50/50 blend composition, the temperature (150°C) at which the interconnected structure is observed in the matrix as well as within the large spherulites is too close to the crystallization temperature (152°C) which was obtained at a cooling rate of 1°C/min, but it is significantly lower than the equilibrium melting temperature of ~175°C. Hence, there is a possibility that a UCST may exist in the present case, as suggested by the observed interconnected SD textures.

The examination of light scattering patterns under both H_v (horizontal polarizer with vertical analyser) and V_v (both polarizers are vertical) conditions reveals a four-lobe clover pattern and a two-fold symmetry pattern, respectively, except for the 10/90 specimen where the V_v pattern is somewhat circular, suggestive of a non-volume filled nature of the system (*Figure 7*). The average diameter of the spherulites as estimated from the H_v peak is comparable with that of the phase separated domains, suggesting that the spherulitic structures develop within these phase-separated domains.

The determination of the exact UCST coexistence points by an optical microscopic investigation is impractical and thus not pursued here simply because of the non-equilibrium nature of the system, where two non-equilibrium processes such as crystallization and phase separation are competing. Moreover, extreme caution should be exercised in determining the coexistence point in any crystalline polymer system because the multiple nucleation often shows the

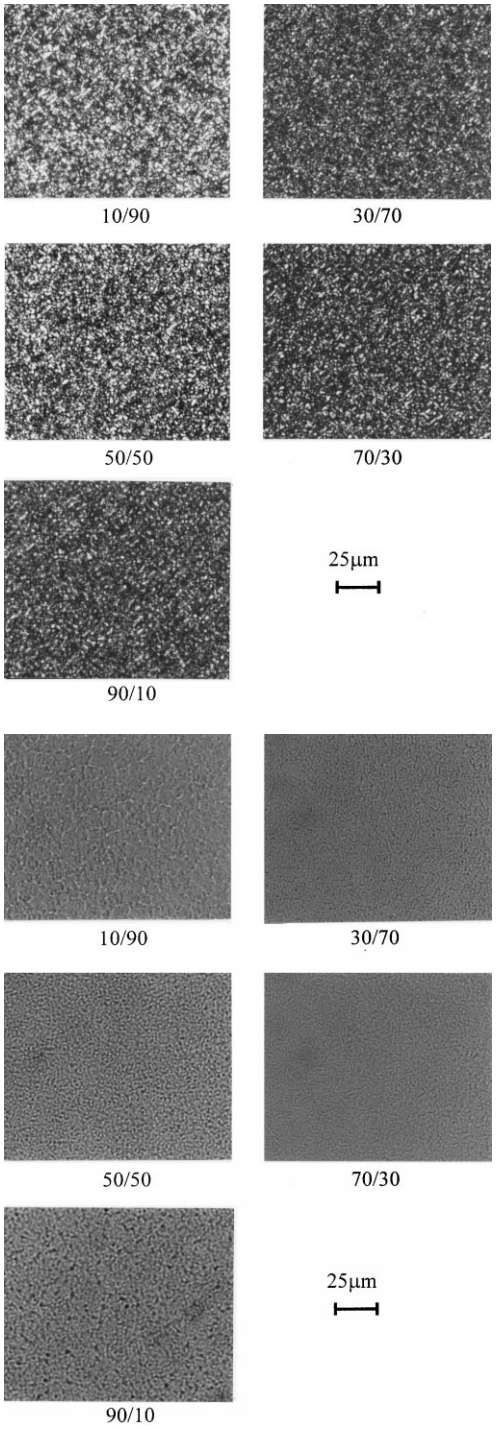

Figure 6 (a) Polarized; and (b) unpolarized optical micrographs obtained at various compositions of the PVF_2/PBA blends after quenching from the isotropic melt at 200°C to ambient temperature

appearance of an interconnected domain texture when it is viewed in the projected basal plane during the microscopic investigation. Although we did not establish an upper critical solution temperature coexistence curve, such a possibility was reported by Tomura *et al.*[12]. The authors demonstrated that a UCST coexistence curve, which indeed occurred below the crystallization temperatures of PVF_2 in its blends with polymethyl methacrylate (PMMA), can be determined by the depolarized light scattering technique.

We should point out a possible paradox regarding the location of the UCST below the crystallization curve of the blends. That is to say, the melting point depression of PVF_2 implies that the interaction parameter (χ) at the crystal

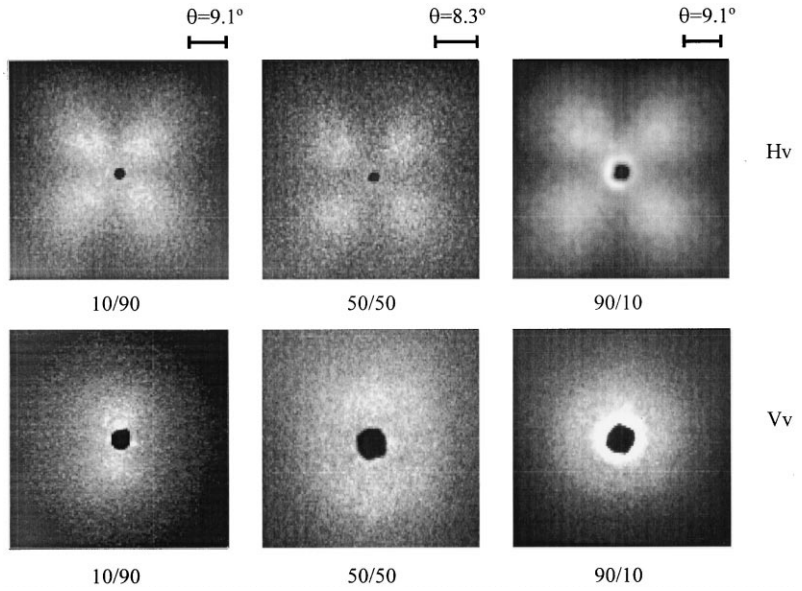

Figure 7 Depolarized H_v and V_v light scattering patterns obtained for various compositions of the PVF_2/PBA blends after quenching from the isotropic melt (200°C) to ambient temperature. θ Represents the scattering angle

melting temperatures must be negative. On the other hand, χ has to be positive in order for the UCST to exist, thereby seemingly inconsistent with the results of the melting point depression. However, it should be borne in mind that both blends (i.e., the PVF_2/PMMA[12] and the present PVF_2/PBA) exhibited the LCST above the melting temperature of PVF_2 where χ is positive. It is quite conceivable that the value of χ changes from positive to negative as the temperature is lowered from the two-phase region (above the LCST) to the isotropic melt (above the crystal melting temperatures). This negative χ may cause the lowering of melting points of PVF_2 in the blends. However, it can reverse its sign again when the temperature is further lowered below the UCST region. In principle, the UCST can exist below the crystallization temperature of one or both components in blends of two crystalline polymers, so long as there is a temperature gap between the crystallization temperatures of the blends and the UCST curve. In the present case, the suggested UCST at low temperatures seemingly contradicts the observed single T_g[1]. However, it should be pointed out that the observed single T_g is too broad to be conclusive. Moreover, the sigmoidal variation of T_g with composition suggests that these T_gs associated with the amorphous phase may be obscured by the interconnectivity with their crystalline structures[1]. Hence, we are unable at present to confirm unambiguously the existence of the UCST below the crystallization temperatures of the PVF_2 constituent.

Crystallization kinetics

The growth of spherulitic structure may be monitored by time resolved light scattering by analysing the H_v scattering maximum. The average radius of spherulites can be estimated according to the Stein–Rhodes equation[9]:

$$\frac{4\pi R}{\lambda}\sin\frac{\theta_{max}}{2} = 4.1 \qquad (1)$$

where R is the average radius of the spherulites, λ and θ are respectively the wavelength of light and scattering angle measured in the medium. Alternatively, the crystallization kinetics may be followed via the small-angle scattering invariant, which can be determined by integrating the scattered intensity over the total scattering volume. The scattering invariant Q for an isotropic system may be given as[13]:

$$Q = \int I(q)\, q^2\, dq \qquad (2)$$

where q is the scattering wavenumber defined as $q = 4\pi/\lambda\sin(\theta/2)$. The light scattering intensity from semicrystalline homopolymers consists of the contributions from density, concentration, and orientation fluctuations. These contributions can be separated through the proper choice of scattering geometries such as the H_v or V_v configurations. The H_v scattering arises exclusively from the orientation fluctuations, whereas the V_v scattering arises due to the differences in concentrations and densities of amorphous and crystal phases, and their orientation fluctuations. In the blends of two-crystalline polymers, orientation fluctuations would prevail in both geometries, in particular the H_v scattering. In the case of random orientation correlation, the invariant functions due to the orientation fluctuations (Q_{orient}) and density fluctuations (Q_{dens}) may be expressed as[13]:

$$Q_{orient} = \int I(q)_{Hv} q^2\, dq \sim \langle\delta^2\rangle \qquad (3)$$

$$Q_{dens} = \int [I(q)_{Vv} - \frac{4}{3} I(q)_{Hv}] q^2\, dq \sim \langle\eta^2\rangle \qquad (4)$$

where $<\delta^2>$ represents mean-square orientation fluctuations and $<\eta^2>$ is the mean-square density or concentration fluctuations. In the absence of density or concentration fluctuations, Q_{orient} can be directly related to the degree of crystallinity. If $<\eta^2>$ has a non-zero finite value, $<\delta^2>$ is no longer equivalent to the bulk degree of crystallinity because the local crystallinity is not constant, but fluctuates over distances comparable with the wavelength of light[13]. Nevertheless, the relative change of $<\delta^2>$ can be considered to represent the changing crystallinity during isothermal crystallization.

From the theoretical consideration presented above, it is evident that time-resolved depolarized (H_v) light scattering can be employed to determine the kinetics of crystallization for several blend compositions at various crystallization

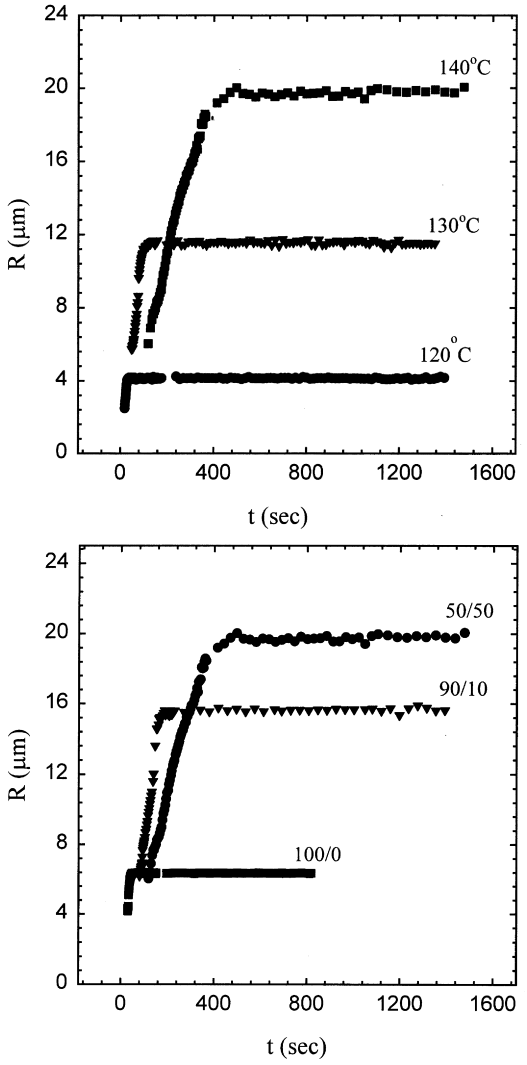

Figure 8 The variation of average radius of the spherulites *versus* elapsed time for: (a) the 50/50 PBF_2/PBA blend at several temperatures; (b) various blend compositions at 140°C

temperatures. The variation of the average radius of the spherulites as estimated from the scattering peaks is plotted against elapsed crystallization time in *Figure 8*. The induction time is generally short and by the time the scattering maximum appears the crystallization process has already advanced considerably. Hence, the influence of the short induction time on the late stage spherulitic growth may not be significant. The plot of *R versus* elapsed time in *Figure 8* reveals the linear relationships in the initial period from which the growth rate can be determined. The observed linear growth rates from the present light scattering experiments are consistent with those reported earlier using the optical microscopic technique[2]. When the spherulitic size reaches its asymptotic value, the present methodology is no longer capable of determining the secondary crystallization, although crystallization is believed to continue internally. The growth rate varies with crystallization temperature depending on the extent of supercooling.

Once the spherulites are impinged, the length scale (size) of the spherulites becomes fixed and most techniques are then incapable of mimicking the continuing crystallization. Therefore, we turned to the H_v scattering invariant approach, as it is capable of detecting the changing crystallinity. In order to extract information regarding the

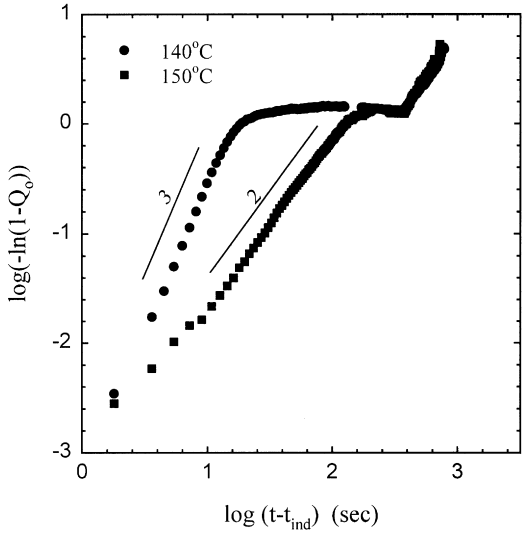

Figure 9 Avrami plots of the scattering invariant versus crystallization time for the pure PVF_2 after quenching from the isotropic melt (200°C) to two different crystallization temperatures

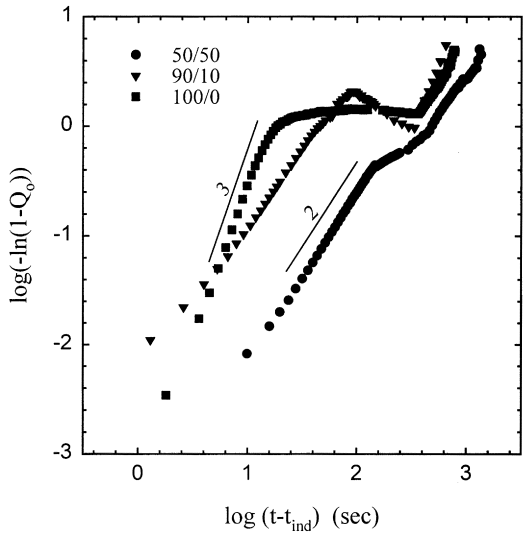

Figure 10 Avrami plot of the scattering invariant *versus* crystallization time for the pure PVF_2, 90/10, and 50/50 PVF_2/PBA blends after quenching from the isotropic melt (200°C) to 140°C

crystallization behaviour from the temporal change of the H_v scattering invariant, the well-known Avrami equation may be used, viz[10,14]:

$$1 - X(t) = \exp(-kt^n) \tag{5}$$

where *X(t)* is the normalized degree of crystallinity, *k* is a rate constant, and *n* is the Avrami exponent which signifies the nature of the nucleation and growth process; e.g., a slope of $n = 3$ suggests that the crystallization of PVF_2 proceeds via three-dimensional growth, while $n = 2$ indicates a two-dimensional growth with athermal nucleation[14]. equation (5) may be rewritten as:

$$\log[-\ln(1 - X)] = \log k + n \log t \tag{6}$$

Since the H_v scattering invariant representing the orientation fluctuation is directly related to the crystallinity, equation (6) may be expressed as:

$$\log[-\ln(1 - Q_o)] = \log k + n \log t \tag{7}$$

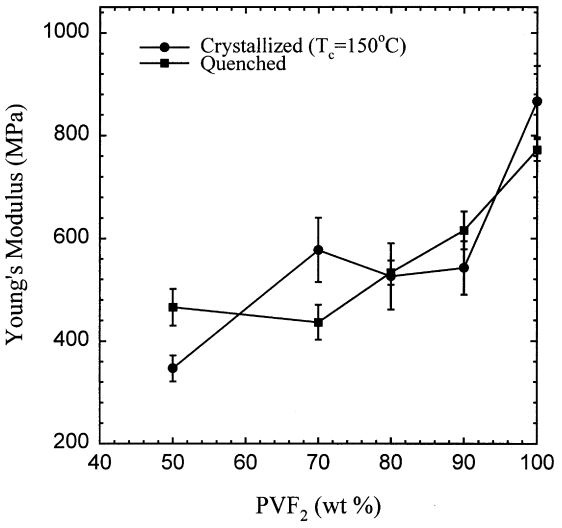

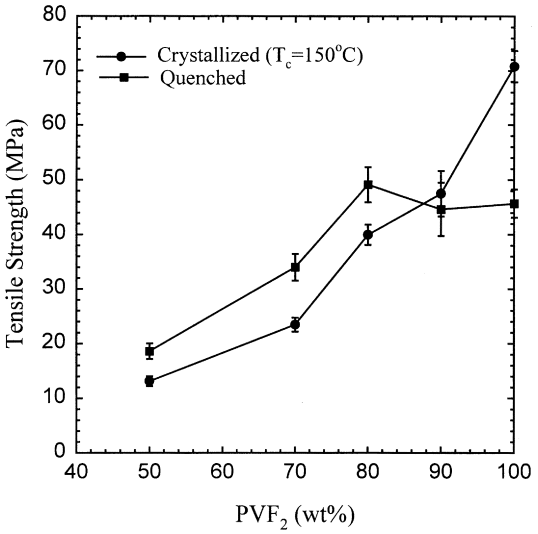

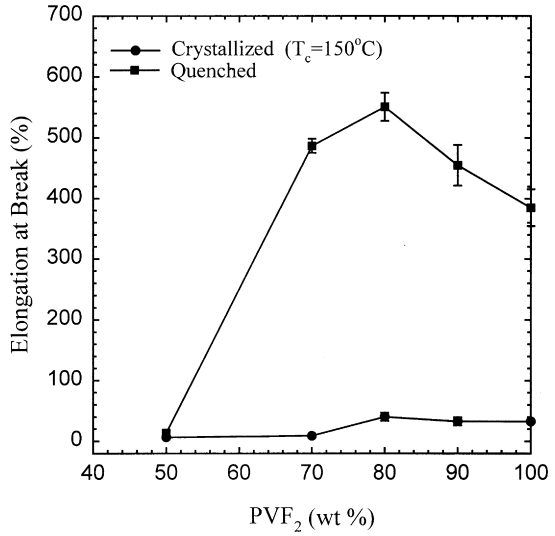

Figure 11 Composition dependence of (a) Young's modulus; (b) tensile strength; and (c) elongation at break for the blends of PVF_2/PBA for two types of specimens prepared by: (i) thermal quenching to room temperature to obtain an interconnected SD structure; and (ii) crystallized at 150°C with spherulitic morphology

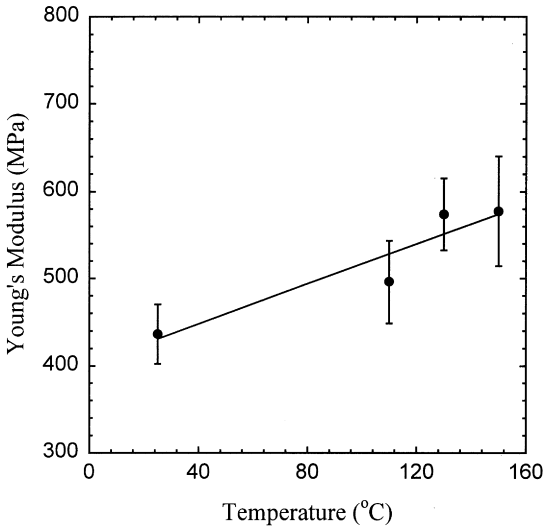

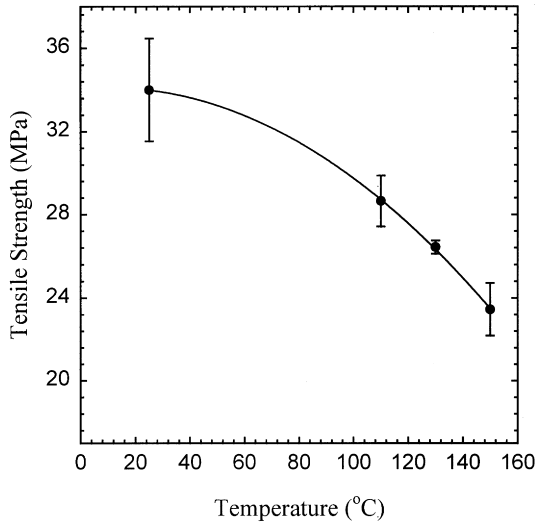

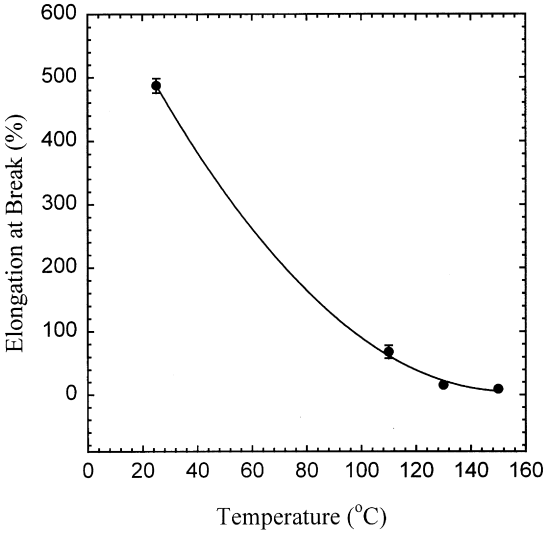

Figure 12 Dependence of (a) Young's modulus; (b) tensile strength; and (c) elongation at break for the blend of 70/30 PVF_2/PBA on various crystallization temperatures, giving rise to different crystalline blend morphologies

where $Q_o = Q_{orient}/Q_{max}$ is the normalized H_v scattering invariant.

The initial crystallization processes such as the evolution of a rod-like and a sheaf-like structure before emerging to a complete spherulite can be readily followed by this scattering invariant approach. Also, it can probe the late stages of crystal growth where secondary crystallization takes place internally within the spherulites. In the Avrami analysis, it is necessary to subtract the induction time from

the total elapsed time in analysing the scattering invariant. Otherwise, the Avrami exponents (slopes) could be erroneously large (about 6–13), which indicates the need for correcting for the induction time. The Avrami plot of the H_v scattering invariant of the pure PVF_2 reveals that the slopes representing the Avrami exponents vary from 2 for the 150°C to 3 for the 140°C quenching (*Figure 9*) indicating a change of two-dimensional to three-dimensional growth. The slope becomes very small during the course of the secondary crystallization, then it increases dramatically for a second time. The second rise in the scattering invariant *versus* time may be related to the formation of a new crystal modification such as the γ type[10]. *Figure 10* shows the Avrami plot for various blends composition during crystallization at 140°C. It is evident that the dimensionality of growth has changed from 3 back to 2 with the addition of PBA component. Concurrently, the spherulitic growth slows down. The second rise in the invariant may be attributed to increased disorder arising from both the concentration fluctuations (contrast between crystal and rejected amorphous phases) and the crystal modification of the PVF_2 in the blends.

Mechanical properties

It has been demonstrated above that the development of phase-separated crystalline blend morphology depends strongly on blend composition and crystallization temperature. We now investigate the relationship between the observed crystalline morphologies and the mechanical properties of these PVF_2/PBA blends. The pure PVF_2 is a ductile material, whereas the neat PBA is a low molecular weight impact modifier without sufficient strength to form a film; thus a tensile test is not possible for the neat PBA.

Young's modulus, tensile strength, and elongation at break were measured by using a Monsanto tensile tester as a function of blend composition (i.e., wt% of PVF_2) prepared under two different methods. The first procedure involves melt-mixing of the dry PVF_2/PBA blends at 210°C for 3–5 min and injection-moulding them in a hot cylindrical mould (~200°C). The samples were quenched to room temperature in order to simulate the blend morphology such as the interconnected SD domain structures, as demonstrated earlier. The melt-mixing and moulding conditions in the second method are the same as those of the first except that the samples were slowly cooled to 150°C and annealed at that temperature in the mould for 1 h in order to generate large spherulitic domains. The blend samples thus prepared by crystallizing at 150°C produce fewer nuclei, thereby allowing crystallization of PVF_2 to proceed until these spherulites reach their limiting sizes.

Figure 11a–c show the variation of Young's modulus, tensile strength and elongation at break as a function of blend composition (i.e., wt% of PVF_2) for two types of specimens mentioned above. The modulus shows an upward trend with increasing PVF_2 content. This behaviour is quite expected because the pure crystalline PVF_2 has a higher crystallinity and a larger modulus value than those of its blends. It can also be anticipated that the neat PVF_2 crystallized at 150°C have a higher crystallinity relative to those prepared by thermal quenching to room temperature, hence higher modulus and higher tensile strength. Another interesting feature is that the elongation at break for the blend compositions crystallized at a high temperature of 150°C is significantly lower than that of the quenched specimens (*Figure 11c*). The tensile strength of the quenched blends shows a similar tendency to that of elongation at break (*Figure 11b*). This observation may be attributed to the enhanced molecular and crystal orientation afforded by the high extensibility of the high PVF_2 blend compositions. This high extensibility is believed to arise from the plasticizing effect of PBA that permits PVF_2 molecules to slide by each other during drawing. The area under the stress–strain curve represents the energy required to break the material, thus it corresponds to the toughness of the materials[15]. These observations indicate that PBA probably acts like an impact modifier for PVF_2. This effect is less obvious for the high temperature crystallized PVF_2/PBA blends having large spherulitic morphology (i.e., crystallized at 150°C) that fail prematurely at the weak spherulitic boundaries.

The dependence of the tensile properties of these PVF_2/PBA blends on crystallization temperature displays interesting behaviour (*Figure 12a–c*). The modulus of the 70/30 PVF_2/PBA increases with increasing crystallization temperature because the degree of crystallinity and the crystal perfection are expected to be higher for the high temperature crystallized blends. Since the modulus is measured in the linear elastic limit (low elongation), the higher crystallinity would exhibit a larger modulus value (*Figure 12a*). However, the elongation at break (*Figure 12c*) and tensile strength (*Figure 12b*), which are measured at the high deformation limits, show the opposite trend because the low temperature crystallization (the larger supercooling) yields the smaller length scale (size) of the imperfect spherulitic structures and thus lower crystallinity. This trend is more accentuated for the thermal quenched blends that have the interconnected SD (bicontinuous) morphology exhibiting higher extensibility and a higher degree of orientation, thereby increased tensile strength. It is fair to conclude that the mechanical properties are strongly dependent on the intricate crystalline blend morphologies afforded by the crystallization habit (crystallization rate, supercooling, etc.) and phase separation (spinodal decomposition, e.g., interconnected bicontinuous structure) behaviour of the crystalline polymer blends. The observed toughness enhancement in the thermal quenched PVF_2/PBA blends is interesting and unique. However, the general validity of the above hypothesis, that is to say the incorporation of the small amount (less than 30 wt%) of the low melting species (e.g., PBA) into the high melting polymer (e.g., PVF_2) in the form of an interconnected SD structure improves the materials' toughness, has yet to be established for other systems.

CONCLUSIONS

We have observed that the emerging crystalline morphology of the PVF_2/PBA blends exhibits a strong dependence on the blend composition and the crystallization temperature. In high PBA-rich compositions such as 10/90, the development of nematic line disclinations was observed, although the PVF_2/PBA blend components themselves contain no identifiable mesogenic groups. This nematic mesophase structure has been attributed to the interaction between the fluoride group of PVF_2 and the ester group of PBA. The possible existence of an upper critical solution temperature (UCST) below the crystallization temperatures of the blends has been suggested, but we did not establish the UCST phase diagram for this PVF_2/PBA blend system due to the strong influence of the crystallization on the coexistence points, e.g., the projection of tiny multiple spherulites can be similar to that of the interconnected SD domains. At present,

we are unable to unambiguously confirm the existence of the UCST because the suggested UCST at low temperatures seemingly contradicts the observed single T_g. However, it should be borne in mind that the observed single T_g is very broad and thus inconclusive. Also, the sigmoidal variation of T_g with composition[1] further suggests that these T_gs may be obscured by the presence of the crystals. It is concluded that the mechanical properties are strongly dependent on the intricate blend morphologies afforded by the crystallization habit, crystalline kinetics, and its competition with phase separation of the crystalline polymer blends. The observed toughness enhancement in the thermal quenched PVF_2/PBA blends is interesting and unique, but its validity for other systems has yet to be established.

ACKNOWLEDGEMENTS

This study was made possible with the partial support of the National Science Foundation, DMR 95-29296 to the University of Akron, and an operating grant to R.St.J.M. from the Natural Science and Engineering Research Council of Canada.

REFERENCES

1. Penning, J. P. and Manley, R. St. J., *Macromolecules*, 1996, **29**, 77.
2. Penning, J. P. and Manley, R. St. J., *Macromolecules*, 1996, **29**, 84.
3. Liu, L. Z., Chu, B., Penning, J. P., and Manley, R. St. J., *Macromolecules*, 1997, **30**, 4398.
4. Tanaka, H. and Nishi, T., *Phys. Rev. Lett.*, 1985, **55**, 1102.
5. Tanaka, H. and Nishi, T., *Phys. Rev. A*, 1989, **39**, 783.
6. Fujita, K., Kyu, T. and Manley, R. St. J., *Macromolecules*, 1996, **29**, 91.
7. Kato, T. and Frechet, J. M., *J. Am. Chem. Soc.*, 1989, **1111**, 8533.
8. Talroze, R. V., Kuptsov, S. A., Sycheva, T. I., Shandryuk, G. A. and Plate, N. A., in *Liquid Crystalline Polymer Systems: Technological Advances*, ed. A. I. Isayev, T. Kyu and S. Z. D. Cheng. ACS Symposium Series 632, Washington D.C., 1995, p. 304.
9. Stein, R. S. and Rhodes, M., *J. Appl. Phys.*, 1961, **31**, 1873.
10. Armistead, K. and Goldbeck-Wood, G., *Adv. Polym. Sci.*, 1992, **100**, 219.
11. Olabisi, O., Robeson, L. M. and Shaw, M. T., *Polymer–Polymer Miscibility*. Academic Press, New York, 1979.
12. Tomura, H., Saito, H. and Inoue, T., *Macromolecules*, 1992, **25**, 1611.
13. Koberstein, J., Russell, T.P. and Stein, R.S., *J. Polym. Sci., Polym. Phys. Ed.*, 1979, **17**, 1719.
14. Wunderlich, B., *Macromolecular Physics*, Vol. 2. Academic Press, New York, 1976.
15. Ward, I. M. and Hadley, D. W., *An Introduction to Mechanical Properties of Solid Polymers*. Wiley, Chichester, 1993.